frontiers in Earth Science

ORIGINAL RESEARCH
published: 06 December 2021
doi: 10.3389/feart.2021.782640

Seasonal Tidal Dynamics in the Qiantang Estuary: The Importance of Morphological Evolution

Dongfeng Xie[1]* *and Zheng Bing Wang*[2,3]

[1]Zhejiang Institute of Hydraulics and Estuary, Hangzhou, China, [2]Faculty of Civil Engineering and Geosciences, Delft University of Technology, Delft, Netherlands, [3]Deltares, Delft, Netherlands

Despite the increasing number of studies on the river-tide interactions in estuaries, less attention has been paid to the role of seasonal morphological changes on tidal regime. This study analyzes the seasonal interplay of river and tide in the Qiantang Estuary, China, particularly focusing on the influences of the active morphological evolution induced by the seasonal variation of river discharge. The study is based on the high and low water levels at three representative stations along the estuary and daily river discharge through 2015, an intermediate flow year in which a typical river flood occurred, as well as the bathymetric data measured in April, July and November, 2015. The results show strong seasonal variations of the water level in addition to the spring-neap variation. These variations are obviously due to the interaction between river discharge and tide but can only be fully explained by including the effect of morphological changes. Two types of the influences of the variation of the river discharge on the tidal dynamics in the estuary can be distinguished: one is immediately induced by the high flow and the other continues for a much longer period because of the bed erosion and the following bed recovery. Tidal range in the upper reach can be doubled after the flood because of bed erosion and then decrease under normal discharge periods due to sediment accumulation. Over a relatively short term such as a month or a spring-neap tidal cycle, there exist good relationships between the tidal range, tidal amplification in the upper reach and the tidal range at the mouth, and between the hydraulic head over the upper and lower reaches. Such relationships are unclear if all data over the whole year are considered together, mainly because of the active morphological evolution.

Keywords: tidal dynamics, morphological evolution, hydraulic head, qiantang estuary, river floods

OPEN ACCESS

Edited by:
Daidu Fan,
Tongji University, China

Reviewed by:
Eduardo Siegle,
University of São Paulo, Brazil
Huayang Cai,
Sun Yat-sen University, China

***Correspondence:**
Dongfeng Xie
dongfeng.xie@hotmail.com

Specialty section:
This article was submitted to Marine Geoscience, a section of the journal Frontiers in Earth Science

Received: *24 September 2021*
Accepted: *22 November 2021*
Published: *06 December 2021*

Citation:
Xie D and Wang ZB (2021) Seasonal Tidal Dynamics in the Qiantang Estuary: The Importance of Morphological Evolution. Front. Earth Sci. 9:782640. doi: 10.3389/feart.2021.782640

INTRODUCTION

An estuary is the transition zone between river environment and the open marine shelf. It represents one of the most profound spatial changes in hydrological and morphological conditions (Dyer, 1997; Dalrymple and Choi, 2007). They favor sectors such as fishery, aquaculture, port and navigation and tourism, often hosting major cities and densely populated areas of great economic importance. Estuaries are also among the most productive ecosystems in the world, with important ecological functions like breeding fish or feeding areas for migratory birds (Kukulka and Jay, 2003; Gao and Wang, 2008). Tidal dynamics is one of the main physical forces for the transport and diffusion processes of sediment, nutrients, pollutions, salinity etc., in estuaries. In the viewpoint of coastal

management, the knowledge of tidal dynamics in an estuary is of major practical significance for navigation, aquatic environment, use of water resources, estuarine ecosystem as well as the planning and design of coastal structures (Jay et al., 2011; Savenije, 2012; Talke and Jay, 2020).

Tidal regimes in estuaries are mainly controlled by the geometry of the estuary (planform and bathymetry), tides from the open sea, river discharge. Changes of tides in estuaries has been ubiquitous worldwide over the past century, in response to natural changes such as sea level rise as well as various human activities (e.g., Pye and Blott, 2014; Du et al., 2018; Talke and Jay, 2020). Studies on the long-term evolution of tides has examined apparent increases in tidal ranges in many estuaries, because human modifications of the estuarine system such as land reclamation, sand extraction, channel dredging, etc., increase the mean depth and reduce hydraulic drag (Wang et al., 2002; Winterwerp et al., 2013; Familkhalili and Talke, 2016; Cai et al., 2018; Ralston et al., 2019). Meanwhile, the seasonal and interannual variations of river discharge also have a significant effect on tidal dynamics in estuaries, particularly in the landward direction where smaller channel cross-sections and tidal prisms prevail (Perillo, 1995; Talke and Jay, 2020). Higher river discharge generates higher water levels, enhances the ebb currents, damps incoming tidal waves, delay wave propagation and alter energy distribution through enhanced friction (e.g., Jay, 1991; Godin, 1999; Sassi and Hoitink, 2013; Zhang et al., 2016). Study in the North Channel of the Changjiang Estuary showed extreme river floods have significant influences on the morphological evolution in the estuary. After a river flood, the estuarine morphology returns to its original state by self-adjusting over decadal timescales (Mei et al., 2018). However, less studies have focused on the influence of seasonal morphological change induced by the natural change such as the variations of river discharge on the tidal dynamics in estuaries, probably because in most estuaries the bed level changes on the seasonal timescale is limited compared with the water depth. There are some estuaries in the world are characterized by active morphological evolutions in the seasonal timescale due to cyclic transition of high and low river discharge (Reddering and Esterhuysen, 1989; Cooper, 2002; Choi et al., 2020). It is necessary to explore the tidal dynamics in an estuary with active morphological changes, especially at the upper reach where the role of river discharge is more significant. The Qiantang Estuary is one of the largest macro-tidal estuaries on the East China Sea coast. It is one of the most morphologically active estuaries worldwide. Local bed level change in several months can be more than 5 m (Chen et al., 1990; Xie et al., 2018). It is also famous for the largest tidal bore worldwide (Bartsch-Winkler and Lynch, 1988; Chanson, 2012). The estuary has been the subject of a number of studies focusing on the provenance of the estuary (Chen et al., 1990; Zhang et al., 2014, 2015), hydrodynamics and sediment transport (Pan and Huang, 2010; Xie and Pan, 2013; Fan et al., 2014, 2016; Tu et al., 2021), the long-term morphodynamic evolutions as well as the morphological responses to human activities (Dai et al., 2014; Liu et al., 2017; Xie et al., 2017a, Xie et al., 2018, Xie et al., 2021a.). Mainly based on the bathymetric and monthly-averaged tidal data in each april, July and November since the 1980s, Xie et al. (2021b) recently found that the interannual natural morphological evolution of the estuary plays an important role on the tidal behaviors. It would be valuable to make a closer analysis of the tidal evolutions due to the seasonal morphological evolution, especially under the influence of episodic river floods which basically occur in every year (Han et al., 2003).

The objective of this study is to explore the seasonal variation of tidal behavior in the Qiantang Estuary, a macro-tidal estuary with active morphological evolution. Specifically, we attempt to delineate the seasonal tidal evolution along the estuary based on measurements in a typical hydrologic year; and to improve our understanding of the role of river discharge and associated morphological changes on tidal regime in estuaries.

STUDY AREA

The Qiantang Estuary is located on the coast of East China Sea, connecting the Hangzhou City to the Hangzhou Bay (**Figure 1**). The Qiantang Estuary - Hangzhou Bay system has a funnel shape with landward decrease in width as well as water depth. The Hangzhou Bay mouth is about 100 km wide with an average depth of about 10 m. At Ganpu, the interface between the Qiantang Estuary and Hangzhou Bay, the width is 18 km with an average depth of 5 m. The width is reduced further landward to approximately 2.5 km at Yanguan and about 1 km at Zakou. A large bar is present in the estuary. The cross-sectionally averaged bed level rises gradually landward from -5 m at (with respect to the Chinese National Vertical Datum of 1985) at Ganpu to above 0 m at Qibao-Cangqian reach, and then falls down to -2 m at Zakou (**Figure 1B**). Sediment in the Qiantang Estuary is mainly composed of well-sorted silt and clay, with the median grain size between 20 and 40 μm, which is mainly from the adjacent Changjiang Estuary (Chen et al., 1990; Xie et al., 2009; Fan et al., 2014; Zhang et al., 2015; Fan et al., 2016; Liu et al., 2018).

The mean tidal range at the Hangzhou Bay mouth is 3.2 m. It is significantly amplified landward by the convergent planform of the estuary. The mean tidal range is around 6.0 m at Ganpu. The tidal waves are seriously deformed upstream (**Figure 2**) and develop into the world's largest tidal bore, the Qiantang bore (Pan et al., 2007). Tidal ranges decrease upstream Ganpu due to bed friction. At Zakou the mean tidal range is about 0.5 m. The annually averaged river discharge of the Qiantang River is 952 m^3/s. The monthly averaged discharges vary between 319 m^3/s and 1705 m^3/s (Xie et al., 2017b). Within a year, the low river discharge occurs from August to next March and the high river discharge occurs from April to July. Up to 60% of the annual runoff occurs from april to July (Han et al., 2003; Xie et al., 2017b). Two factors control the occurrence of high river discharge: monsoon climate and typhoon events (Han et al., 2003). During a river flood, the discharge rises and falls sharply in

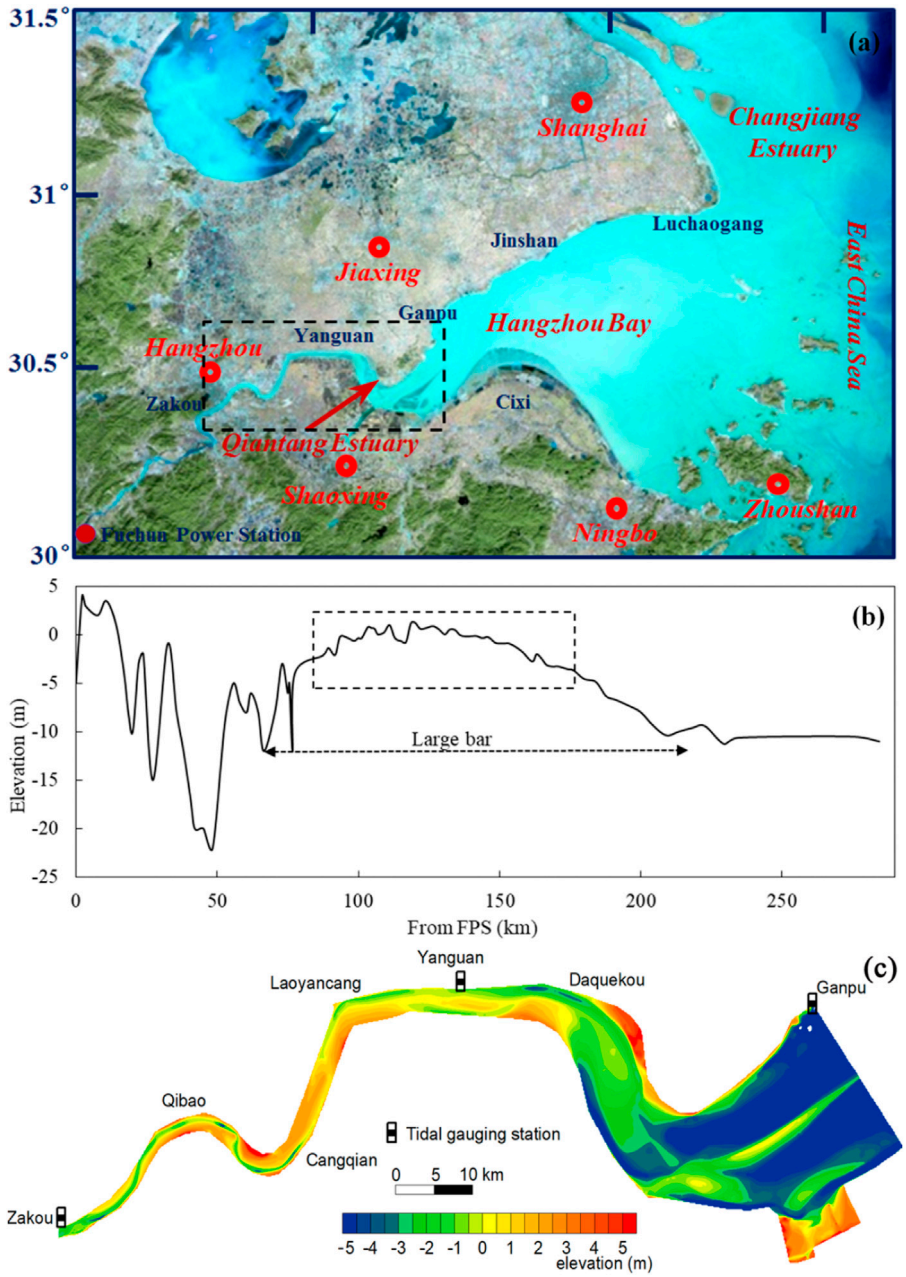

FIGURE 1 | (A) Location of the Qiantang Estuary, **(B)** the lateral-averaged longitudinal profile along the estuary and **(C)** bathymetry of the Qiantang estuary in april 2015. Panels b and c are after Xie et al. (2017b) and Xie et al. (2018), respectively. The dashed line in panels **(A)** and **(B)** denote the Qiantang Estuary.

several or more than 10 days, and the peak discharge can be more than 10000 m^3/s.

Data and Methods

In this study three types of field data have been collected. The high and low water levels at Ganpu, Yanguan and Zakou tidal gauging stations in 2015 and the daily river discharge from Fuchun power station (FPS) in the same period are collected from Zhejiang Hydrographic Office, and the bathymetrical data in April, July and November, 2015 are collected from Zhejiang Surveying Institute of Estuary and Coast. The three tidal stations are located at the seaward end, the middle and the landward end of the estuary, respectively. The average discharge in 2015 is 943 m^3/s, comparable with the long-term average. The river discharge fluctuated around 600 m^3/s in most time of the year. During 5–27 June a river flood occurred with the peak discharge being 12600 m^3/s (**Figure 3A**). The bathymetry was surveyed using an Odom Hydrotrac echo-sounder that gives the vertical error of less than 0.1 m, and a global positioning system (GPS) by Trimble that gives the positioning error within 1 m.

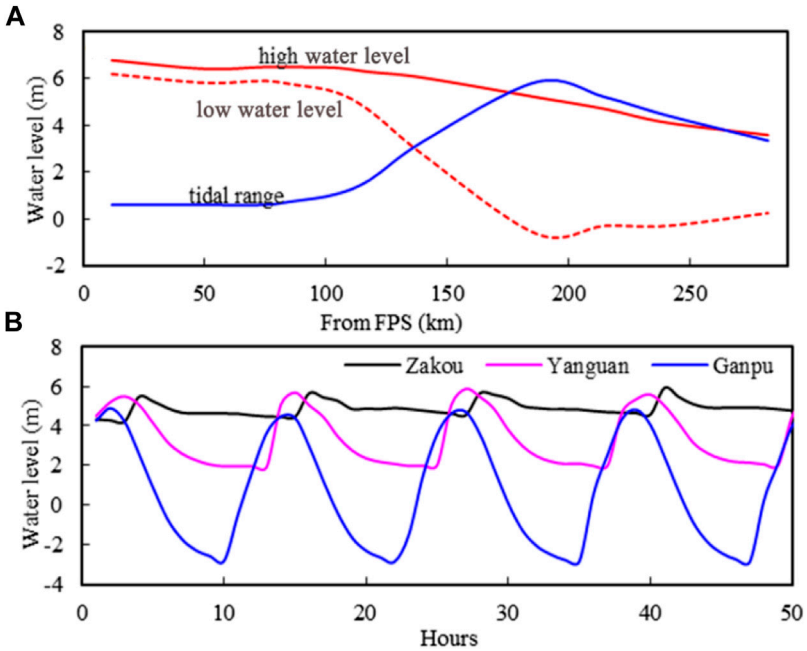

FIGURE 2 | Multi-year averaged high and low water levels and tidal range along the estuary **(A)**, and an example of the time series of water levels at the Zakou, Yanguan and Ganpu stations during spring tide in September 2015 **(B)**.

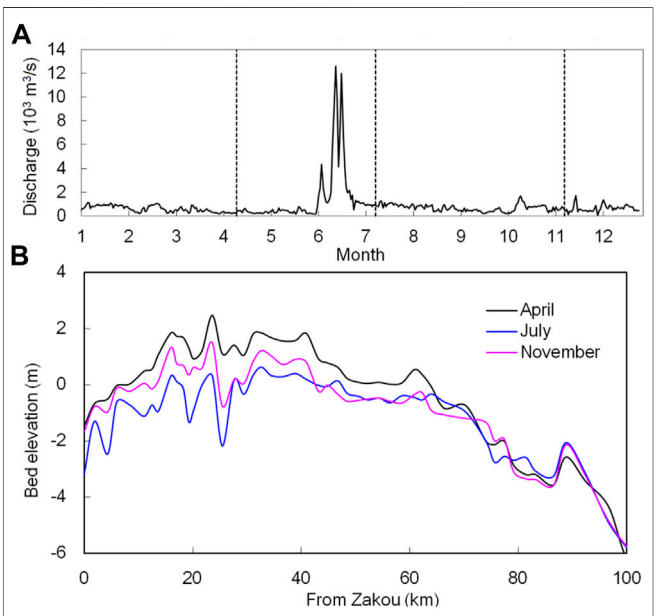

FIGURE 3 | Time series of daily river discharge in 2015 **(A)** and the cross-sectional bed level along the estuary in april, July and November of 2015 **(B)**. The dashed lines in panel **(A)** denote the bathymetric survey periods. Panels a is after Xie et al. (2018).

The tidal range per lunar day is calculated as the difference between high and low water levels (both calculated as the average of two consecutive values). Tidal amplification factor is calculated following Wang et al. (2019):

$$F_{Zakou} = A_{Zakou}/A_{Ganpu} \quad (1)$$

$$F_{Yanguan} = A_{Yanguan}/A_{Ganpu} \quad (2)$$

where F is the amplification factor, A is tidal range, and the subscripts denote the tidal stations. This way of analysis has some similarity with the admittance method (Munk and Cartwright, 1966). Instead of using the astronomical potential in the admittance method, the measured tide at the mouth of the estuary is used as reference. Any change in time of this parameter is an indication for changes in the physical conditions in the estuary. It favors identifying any sudden changes as it provides tide to tide variations.

Moreover, the hydraulic heads over the upper (Zakou - Yanguan) and lower (Yanguan - Ganpu) reaches are determined as the differences between the mid-tides at the upstream and downstream stations. The mid-tide is an average of high and low water levels. The direct cause of the hydraulic head is the river discharge. This parameter can provide another indication of the physical condition of the estuary.

RESULTS

Morphological Evolution

As water levels in the Qiantang Estuary are strongly influenced by the bed level changes, it is necessary to analyze firstly the bathymetrical changes. The morphological evolutions in 2015 have been reported by Xie et al. (2018). They found that the dynamic equilibrium

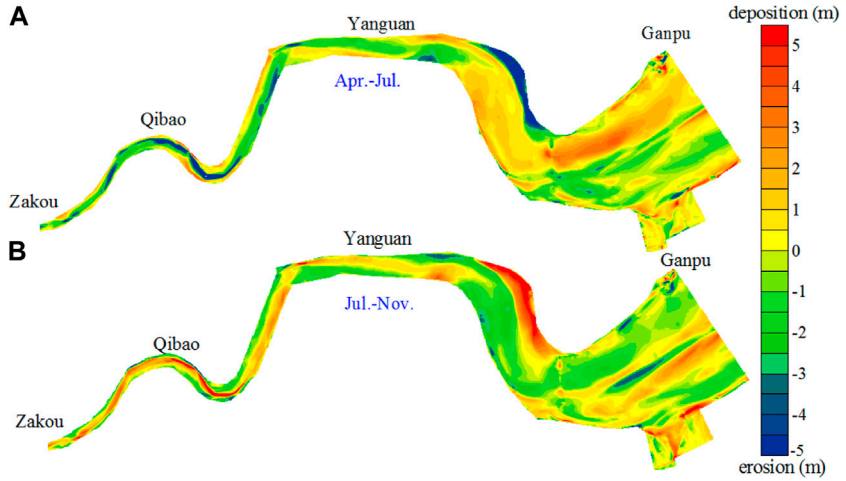

FIGURE 4 | Bed erosion and accretion patterns from april to July **(A)** and from July to November **(B)** in 2015 (after Xie et al., 2018).

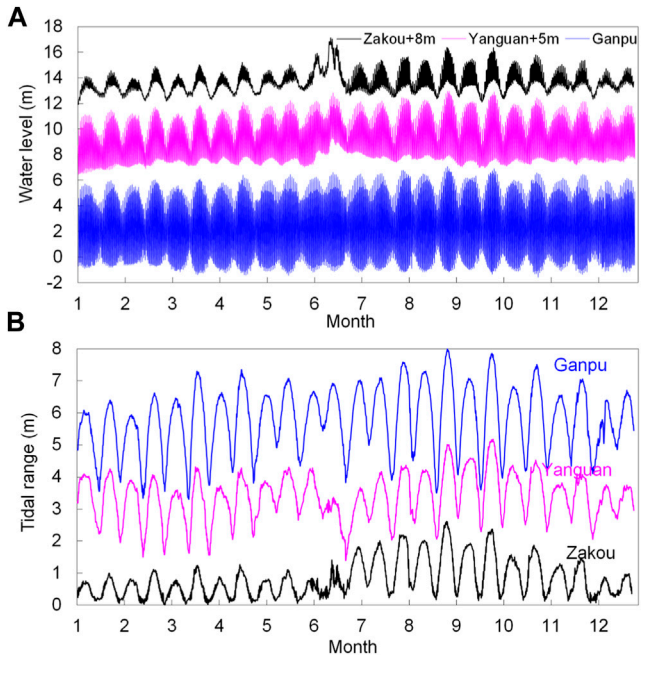

FIGURE 5 | Time series of water levels **(A)** and tidal ranges **(B)** at Zakou, Yanguan and Ganpu in 2015.

in the estuary is controlled by two extreme hydrographic conditions: tidal bore and river floods. Xie et al (2021b) found since the 1980s the tidal ranges at Zakou and Yanguan correlate well with the channel volume of the Zakou-Laoyancang (ZL) and Laoyancang-Daquekou (LD) reaches. For reasons of clarity, the following paragraphs present a short reanalysis of the morphological evolutions and provide a basis for the analysis of tidal dynamics.

Between april and July of 2015, both of the ZL and LD reaches underwent erosion (**Figures 3B**, **4**).The cross-section averaged bed level of the two reaches lowering about 0.81 and 0.06 m, respectively. Accordingly the channel volumes below the local high water level over the two reaches enlarged from 224 × 10^6 and 203 × 106 m^3 in april to 333 × 10^6 and 241 × 106 m^3 in July, respectively, indicating increases of 109 × 106 m^3 and 38 × 106 m^3. The erosion of the ZL reach was more significant that the LD reach. Apparently, the erosion was caused by the river flood in June, because the discharge prior to the river flood was smaller than the bed formation discharge of the estuary, 1,100 m^3/s (Chen et al., 2006; Xie et al., 2017b). The eroded sediment was transported and accumulated seawards, resulting in a bed aggradation of about 0.04 m at the Daquekou-Ganpu (DG) reach. The channel volume below the local high water level over the DG reach decreased from 2,633 × 10^6 in April to 2,542 × 106 m^3 in July, indicating a decrease of 91 × 106 m3.

The bed level change between July and November was opposite. Sediment accumulation and erosion occurred in the ZL reach and DG reach, respectively, because the tides, especially the tidal bore, can transport a large amount of sediment from the lower reach landward (Chen et al., 1990; Han et al., 2003; Xie et al., 2018). The channel volume over the ZL reach was 280 × 106 m^3 in November, indicating a decrease of 53 × 106 m^3 from July to November; whereas the channel volume over the DG reach was 2,565 × 106 m^3 in November, increased by 24 × 106 m^3 in the same period. The channel volume change over the LD reach was insignificant, being 247 × 106 m3, only 6 × 106 m^3 larger than that in July.

Water Levels and Tidal Ranges

Water levels and tidal ranges at the three stations are characterized by spring-neap tidal cycles (**Figure 5**). The monthly lowest low level and highest high level at Ganpu varied between −1.58 m and −0.62 m and between 5.52 m and 7.07 m, respectively. The tidal range at this station was

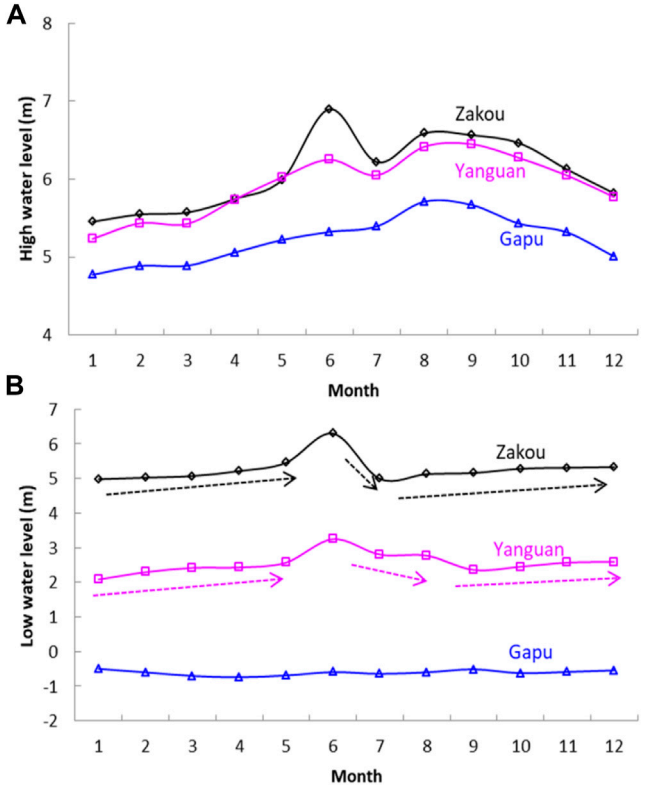

FIGURE 6 | Monthly averaged high **(A)** and low **(B)** water levels at Zakou, Yanguan and Ganpu Station in 2015.

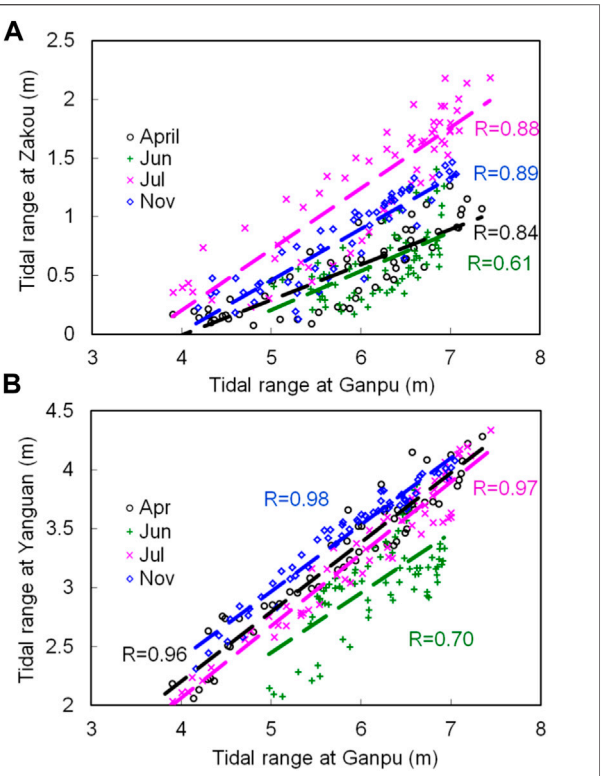

FIGURE 7 | The relationships between the tidal range at Zakou **(A)** and Yanguan **(B)** and that at Ganpu.

relatively small during the first 2 months of the year, less than 6.5 m during spring tides. It increased in the following months and reached the maximum in September with the maximum during spring tides being 7.89 m. Then it decreased in the last months, with the maximum being 6.63 m during December. This is related to the seasonal variation of the incoming tide from the Hangzhou Bay mouth (Editorial Committee for Chinese Harbors and Embayment (ECCHE), 1992). At Yanguan the monthly highest high level varied between 6.13 and 7.98 m, but low water level shows less difference between spring and neap tides fluctuating between 1.46 and 2.63 m, except during the river flood when it was 3.65 m. The tidal range varied between 2.62 and 5.18 m. At Zakou a remarkable characteristic is that the low water level during spring tides was higher than during neap tides. For example, from January to May, the monthly lowest low water level during spring and neap tides were 5.02–5.79 m and 4.18–5.17 m, with the former about 0.7 m higher than the latter. This is because the volume of freshwater retained in the inner reach during spring tides is larger, thus raising the mean water level (Godin, 1999). The tidal range at Zakou varied between 0.04 and 1.40 m.

During the river flood, the water levels at Zakou and Yanguan increased to 2.1 and 0.7 m above the normal high water levels of spring tides, respectively (**Figure 5A**). Tidal range at Yanguan was apparently decreased, indicating the incoming tide was constrained by the high river discharge (**Figure 5B**). However, the decrease of tidal range at Zakou during the river flood was unobvious. Immediately after the river flood, the low water level at Zakou decreased by about 0.5 m. As a result, the tidal range at Zakou increased significantly. Whereas the tidal range at Yanguan is immediately recovered to that before the river flood. Overall, the influence of river flood on the water levels at Ganpu was insignificant.

Figure 6 shows the monthly averaged high and low water levels at the three stations. The high water level at Ganpu increased from January to September and then decreased in the next months. The seasonal variations of the high levels at Zakou and Yanguan were consistent with Ganpu, except that the river flood in June caused significant increase in the high water levels. The monthly low water level at Ganpu was more or less a constant, fluctuating around −0.6 m. Both the monthly low water levels at Zakou and Yanguan showed a slow increase trend during the periods without the river flood. For example, from January to May the low water level at Zakou increased from 4.98 to 5.45 m; this process was disturbed by the river flood which lowered the monthly averaged low water level by 0.46 m, and then the low water level increased again gradually from 4.99 to 5.33 m from July to December.

Figure 7 depicts the relation between the tidal ranges at Ganpu and at the two upstream stations in April, July, November and June, representing the periods before and after the river flood,

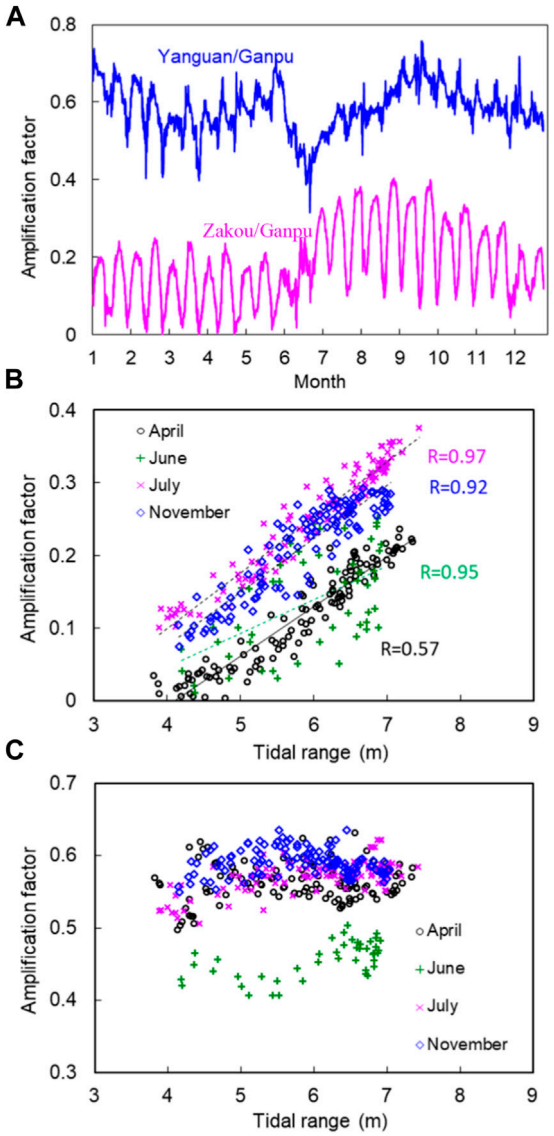

FIGURE 8 | Time series of tidal amplification factors at Zakou and Yanguan **(A)**, and their relationships with the tidal range at Ganpu **(B, C)**.

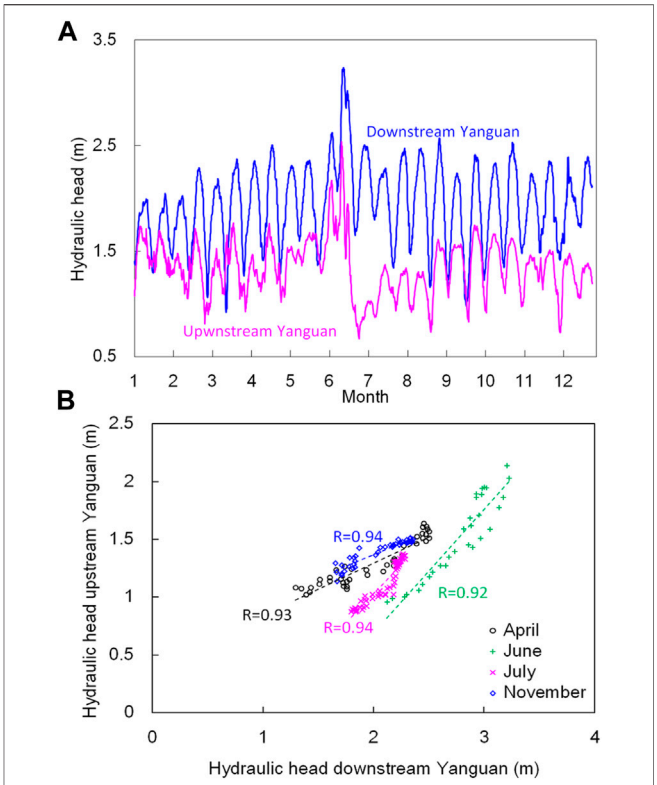

FIGURE 9 | Time series of the hydraulic heads over the upper and lower reaches **(A)**, and their relationships **(B)**.

after the period of large tidal range in Autumn and during the river flood. If all data through the entire year are considered, the relations between the tidal ranges at Ganpu and at the two upstream stations show insignificant correlation. However, good relationships existed during a relative short period. Under the same tidal range at Ganpu, the tidal range at Zakou was largest in July, and smaller in June. The monthly variation of the relationships can only be explained by the bathymetrical changes within the estuary, because in such an analysis the influence of the tidal range at Ganpu has been excluded and the river discharges in most months are comparable. At Yanguan, the difference of the relations among months are smaller except that the tidal range was apparently damped by the high flow in June.

Tidal Amplification

Figure 8A illustrates the time series of the tidal amplification factors at Zakou and Yanguan. The factor at Zakou shows clear spring-neap tidal cycles, varying between 0.01 and 0.41. In the months before the river flood, the factor at Zakou is relatively small, with the average being 0.12. During the period of the river flood, the spring-neap cycle of the amplification was interrupted and the correlation between the factor and the tidal range at Ganpu was weakened. After the river floods, the amplification factor was increased significantly. The average in July was 0.22, almost doubled of that before the river flood. The amplification factor increased further until September in which the average was 0.28, and then decreased gradually to be around 0.15, comparable with that in the first 2 months in 2015. The correlation between the amplification factor at Zakou and the tidal range at Ganpu was insignificant if all data in the whole year of 2015 are considered. However, good relationship exists for a relatively short period, for example 1 month as shown in **Figure 8B**.

The amplification factor at Yanguan varied between 0.32 and 0.76, with an average of 0.58. Its spring-neap cycle was unclear except that a low factor can be detected at neap tides. During the river floods the factor at Yanguan was decreased significantly, indicating that the high river discharge damped the tides. The bed level change at the lower reach induced by

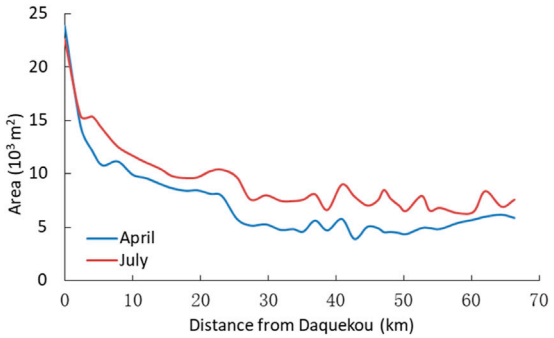

FIGURE 10 | The cross-sectional areas upstream Daquekou before and after the river flood.

the flood was less than in the upper estuary (**Figures 3B**, **4**), hence the influence of the morphological change at Yanguan reach was relatively small. Unlike the good relationship between the tidal ranges at Yanguan and Ganpu, the amplification factor at Yanguan seems hardly influenced by the tidal range at Ganpu. For example, the factor at Yanguan fluctuates around 0.55 in april, July and November (**Figure 8C**).

Hydraulic Head

The hydraulic heads also show spring-neap tidal cycles (**Figure 9A**). In 2015 they varied between 0.87 and 2.74 m in the upper reach and between 0.92 and 3.24 m in the lower reach, respectively. This indicates that the water surface slope in the lower reach was larger than in the upper reach, because the lengths of both reaches are comparable. Usually water surface slopes in estuaries increase in the landward direction because of the backwater effect (e.g., LeBlond, 1978; Godin and Martinez, 1994). The abnormal spatial distribution of the water slopes in the Qiantang Estuary is related to the unique longitudinal bathymetric profile (**Figure 1B**). The drastic rise of the bed elevation in the lower reach increases the low water level significantly, and thus increases the tidally averaged water level.

Hydraulic heads over both reaches increased obviously during the river flood in June due to the backwater effect. After the river flood, the hydraulic head over the lower reach recovered immediately, but over the upper reach it lowered by about 0.8 m. The difference between the hydraulic head changes over the two reaches is probably related to the spatial difference of the bed level changes. The bed erosion by the flood in the upper reach was 1–3 m, which lowered the water level significantly. The bed level change and the corresponding change in water levels in the lower reach are less. If all data through the whole year were considered, the relationship between the hydraulic heads over the two reaches is unclear, indicating the active morphological changes. However, in a relatively short period, good correlation does exist (**Figure 9B**). For a relatively short period, the bed level changes were minor. Then the hydraulic heads over both reaches mainly depend on the tidal forcing at the seaside.

DISCUSSION AND CONCLUSIONS

The seasonal tidal behavior in the Qiantang Estuary has been explored here in order to determine the impact of the variation of the river discharge, particularly considering the active morphological evolution. One of the most important findings in this study is that the active morphological evolution in the Qiantang Estuary induced by the river flood has significant feedback on tidal dynamics, especially in the upper estuary. The river flood caused significant bed erosion. It also increased the water levels and damped the incoming tides at Yanguan where the bed evolution was relatively small (**Figures 5–8**). However, the decrease of tidal range at Zakou during the river flood was insignificant. The tidal dynamics near Zakou depends on the relative balance between channel convergence and bottom friction (Garel and Cai, 2018; Cai et al., 2020). The convergence length can be calculated based on the cross-sectional area along the estuary $\bar{A}$:

$$\bar{A} = \overline{A_0} \exp(-x/a) \tag{3}$$

where $\overline{A_0}$ is the cross-sectional area at Daquekou, x is the distance from Daquekou and the constant a is the convergence length of the cross-sectional area. **Figure 10** shows the cross-sectional area upstream Daquekou before and after the river flood. After the flood, the area upstream Daquekou increased significantly, with the averaged increase being 2.13 × 103 m3. Correspondingly, the convergence length increased by about 50%, from 44.3 to 66.2 km. As the width is fixed after the embankment project, the calculated convergence reflects the longitudinal change of the water depth. Then the tidal amplification increases with the increase of the convergence length (Garel and Cai, 2018). This effect counteracts the tidal damping by high river flow. After the river flood, the eroded bed lowered the local low water level, increased the water depth and decreased the bed friction, hence the tidal range was doubled (**Figures 5–8**).

The seasonal change in the amplification factor at Zakou is much larger than many other estuaries (Jalón-Rojas et al., 2018; Wang et al., 2019) where the correlation between the amplification factor at the upper estuary and the tidal range at the mouth is relative stable over decades. Furthermore, the tidal amplification is larger during spring tide than during neap tide (**Figure 8**), in agreement with the findings of Xie et al. (2018) based on the monthly-averaged data since the 1980s. This is different from other tide-dominated estuaries such as the Guadalquivir Estuary in the Spain (Wang et al., 2014), Garonne tidal river in the France, (Jalón-Rojas et al., 2018), the Guadiana estuary in the Portugal (Garel and Cai, 2018) and the LingdingYang Bay in the Pearl River Estuary of China (Cai et al., 2020). This is related to the landward increase of water depth due to the presence of the large bar (**Figure 1B**) which decreases the friction effects and the high sediment concentration which reduces the hydraulic drag (Xie et al., 2021b).

The tidal amplification induced by bed erosion during the river floods in the Qiantang Estuary is similar to the tidal amplification induced by human activities in many other

estuaries. For example, the tidal range at Dendermonde, the Upper Scheldt Estuary increased from 3.2 to 3.6 m in 1970s to 4.0–4.5 m in 2010s triggered by deepening or narrowing of the estuary (Wang et al., 2019); the tidal range in the lower Loire Estuary, France increased from 1.2 m in 1904 to 5.5 m in 2004, amplified by 3.6 times, due to progressive narrowing of the estuary (Winterwerp et al., 2013); gravel extraction in the upper Garonne River, France, during 1953 and 1994 amplified the tidal range by 23% (Jalón-Rojas et al., 2018); the tidal amplitude in the upper Hudson Estuary has more than doubled since the late 19th century due to channel deepening (Ralston et al., 2019); the annual tidal ranges at Shanshui and MK stations in the upper Pearl River Delta, China increased rapidly from around 0.25 m before 1990 to around 0.6 m in 201 0 due to large-scale sand excavation (Cai et al., 2016). The tidal amplification induced by human activities is usually irreversible and a regime shift to more dynamic and high turbidity has developed in the systems (Winterwerp et al., 2013; Van Maren et al., 2015; Jalón-Rojas et al., 2018; Wang et al., 2019). The tidal amplification in the present study can be decreased during low river discharge period because of sediment accumulation. Several studies have focused on the role of seasonal variations of river discharges on the estuarine morphological evolutions (Reddering and Esterhuysen, 1989; Cooper, 2002; Choi et al., 2020). Unfortunately, so far no study has been reported on the seasonal tidal dynamics due to seasonal morphological evolution. The results in this study revealed that the tidal amplification in the estuary can be decreased during the low river discharge periods because of sediment accumulation. This is also relevant to other similar estuaries worldwide.

The mean tidal discharge at Ganpu is in an order of 105 m3/s (Chen et al., 1990; Huang et al., 2021), two orders larger than the normal river discharge. Under normal discharge conditions, the estuary is flood-dominant (Xie et al., 2018). In particular, the tidal bore in the Qiantang Estuary is an extreme hydrographic condition. During spring tides, maximum velocity at the bore arrival can be 5–6 m/s, inducing a large sediment transport capacity. During a spring-neap cycle the net sediment transport through the Yanguan transect can be 8,000 m^3 landwards (Xie et al., 2018). Hence during normal discharge period, the upper estuary is in a state of sediment accumulation, as indicated by the slowly increase in the monthly low water levels at Zakou and Yanguan in **Figure 6B**. Correspondingly, the tidal range and tidal amplification decrease gradually (**Figures 7**, **8**). Using a long time series of bathymetrical data in each April, July and November since the 1960s and the water level records in the same period, Han et al. (2003) found that the low water level in the upper Qiantang Estuary depends on local bed elevations. However, it is difficult to survey the bathymetry in the Qiantang Estuary with a frequency higher than three times per year due to financial and logistic reasons. The time series of the increasing monthly averaged low water levels herein can provide evidence of higher temporal resolution to support how the upper estuary is gradually accumulated in normal river discharge periods.

Based on the results in the present study, two types of the responses of the tidal behavior to the variation of the river discharge can be distinguished: short-term response during the high river discharge and longer-term response related to the tidal forcing from the open sea. During the periods of river floods, both water level and hydraulic head increased significantly (**Figures 5**, **6**, **9**). After the river floods, the lowered bed level can be recovered gradually in the following months due to the landward sediment transport by the tides. Accordingly, the low water level and hydraulic head increased and the tidal range decreased.

DATA AVAILABILITY STATEMENT

The original contributions presented in the study are included in the article/Supplementary Material, further inquiries can be directed to the corresponding author.

AUTHOR CONTRIBUTIONS

DX: Conceptualization, formal analysis, Writing-original draft and funding acquisition. ZBW: Methodology, data analysis and writing-Review and editing. All authors contributed to the article and approved the submitted version.

FUNDING

This research was financed by the National Natural Science Foundation of China (No. 41676085; 42176170), Zhejiang Provincial hydraulic science and technology planning project (RB2033), Zhejiang Provincial Natural Science Foundation of China (No. LY20E090001).

ACKNOWLEDGMENTS

We are grateful to Chengfei Hu for his assistance with data processing.

REFERENCES

Bartsch-Winkler, S., and Lynch, D. K. (1988). *Catalog of Worldwide Tidal Bore Occurrences and Characteristics*, 1022. Denver: USGS Circular, l17.

Cai, H., Savenije, H. H. G., Jiang, C., Zhao, L., and Yang, Q. (2016). Analytical Approach for Determining the Mean Water Level Profile in an Estuary with Substantial Fresh Water Discharge. *Hydrol. Earth Syst. Sci.* 20, 1177–1195. doi:10.5194/hess-20-1177-2016

Cai, H., Huang, J., Niu, L., Ren, L., Liu, F., Ou, S., et al. (2018). Decadal Variability of Tidal Dynamics in the Pearl River Delta: Spatial Patterns, Causes, and Implications for Estuarine Water Management. *Hydrol. Process.* 32 (25), 3805–3819. doi:10.1002/hyp.13291

Cai, H., Zhang, P., Garel, E., Matte, P., Hu, S., Liu, F., et al. (2020). A Novel Approach for the Assessment of Morphological Evolution Based on Observed Water Levels in Tide-Dominated Estuaries. *Hydrol. Earth Syst. Sci.* 24, 1871–1889. doi:10.5194/hess-24-1871-2020

Chanson, H. (2012). *Tidal Bores, Aegir, Eagre, Mascaret, Pororoca: Theory and Observations*. Singapore: World Science.

Chen, J. Y., Liu, C. Z., Zhang, C. L., and Walker, H. J. (1990). Geomorphological Development and Sedimentation in Qiantang Estuary and Hangzhou Bay. *J. Coast. Res.* 6 (3), 559–572.

Chen, S. M., Han, Z. C., and Hu, G. J. (2006). Impact of Human Activities on the River Reach in the Qiantang Estuary. *J. Sed. Res.* (4), 61–67 [in Chinese with English abstract]. doi:10.1007/s11434-006-2076-2

Choi, K., Kim, D., and Jo, J. (2020). Morphodynamic Evolution of the Macrotidal Sittaung River Estuary, Myanmar: Tidal Versus Seasonal Controls. *Mar. Geol.* 430, 106367. doi:10.1016/j.margeo.2020.106367

Cooper, J. A. G. (2002). The Role of Extreme Floods in Estuary-Coastal Behaviour: Contrasts between River- and Tide-Dominated Microtidal Estuaries. *Sediment. Geol.* 150, 123–137. doi:10.1016/S0037-0738(01)00271-8

Dai, Z.-j., Liu, J. T., Xie, H.-l., and Shi, W.-y. (2014). Sedimentation in the Outer Hangzhou Bay, China: the Influence of Changjiang Sediment Load. *J. Coastal Res.* 298, 1218–1225. doi:10.2112/jcoastres-d-12-00164.1

Dalrymple, R. W., and Choi, K. (2007). Morphologic and Facies Trends through the Fluvial-marine Transition in Tide-Dominated Depositional Systems: A Schematic Framework for Environmental and Sequence-Stratigraphic Interpretation. *Earth-Science Rev.* 81 (3-4), 135–174. doi:10.1016/j.earscirev.2006.10.002

Du, J., Shen, J., Zhang, Y. J., Ye, F., Liu, Z., Wang, Z., et al. (2018). Tidal Response to Sea-Level Rise in Different Types of Estuaries: The Importance of Length, Bathymetry, and Geometry. *Geophys. Res. Lett.* 45, 227–235. doi:10.1002/2017GL075963

Dyer, K. R. (1997). *Estuaries - Physical Introduction*. Chichester: John Wiley & Sons.

Editorial Committee for Chinese Harbors and Embayment (ECCHE) (1992). *Chinese Harbors and Embayment (Part V)*. Beijing: China Ocean Press. Chinese.

Familkhalili, R., and Talke, S. A. (2016). The Effect of Channel Deepening on Tides and Storm Surge: A Case Study of Wilmington, NC. *Geophys. Res. Lett.* 43 (17), 9138–9147. doi:10.1002/2016GL069494

Fan, D., Tu, J., Shang, S., and Cai, G. (2014). Characteristics of Tidal-Bore Deposits and Facies Associations in the Qiantang Estuary, China. *Mar. Geology.* 348, 1–14. doi:10.1016/j.margeo.2013.11.012

Fan, D., Tu, J., Shang, S., Chen, L., and Zhang, Y. (2016). "Morphodynamics and Sedimentary Facies in a Tidal-Fluvial Transition with Tidal Bores (The Middle Qiantang Estuary, China)," in *Contribution to Modern and Ancient Tidal Sedimentology: Proceedings of the Tidalites 2012 Conference*. Editors B. Tessier and J.Y. Reynaud (IAS Special Publication), 48, 75–92. doi:10.1002/9781119218395.ch5

Gao, S., and Wang, Y. P. (2008). Changes in Material Fluxes from the Changjiang River and Their Implications on the Adjoining continental Shelf Ecosystem. *Cont. Shelf Res.* 28 (12), 1490–1500. doi:10.1016/j.csr.2007.02.010

Garel, E., and Cai, H. (2018). Effects of Tidal-Forcing Variations on Tidal Properties along a Narrow Convergent Estuary. *Estuaries Coasts* 41 (7), 1924–1942. doi:10.1007/s12237-018-0410-y

Godin, G., and Martinez, A. (1994). Numerical Experiments to Investigate the Effects of Quadratic Friction on the Propagation of Tides in a Channel. *Cont. Shelf Res.* 14 (7-8), 723–748. doi:10.1016/0278-4343(94)90070-1

Godin, G. (1999). The Propagation of Tides up Rivers with Special Considerations on the Upper Saint Lawrence River. *Estuarine, Coastal Shelf Sci.* 48, 307–324. doi:10.1006/ecss.1998.0422

Han, Z. C., Dai, Z. H., and Li, G. B. (2003). *Regulation and Exploitation of Qiantang Estuary*. Beijing: China Water Power Press. in Chinese.

Huang, J. B., Sun, Z. L., and Xie, D. (2021). Morphological Evolution of a Large Bar in the Qiantang Estuary, China, since 1960s. *Acta Ocean. Sin.* accepted.

Jalón-Rojas, I., Sottolichio, A., Hanquiez, V., Fort, A., and Schmidt, S. (2018). To what Extent Multidecadal Changes in Morphology and Fluvial Discharge Impact Tide in a Convergent (Turbid) Tidal River. *J. Geophys. Res. Oceans* 123, 3241–3258. doi:10.1002/2017JC013466

Jay, D. A., Leffler, K., and Degens, S. (2011). Long-term Evolution of Columbia River Tides. *J. Waterway, Port, Coastal, Ocean Eng.* 137 (4), 182–191. doi:10.1061/(ASCE)WW.1943-5460.0000082

Jay, D. A. (1991). Green's Law Revisited: Tidal Long-Wave Propagation in Channels with strong Topography. *J. Geophys. Res.* 96, 20585–20598. doi:10.1029/91JC01633

Kukulka, T., and Jay, D. A. (2003). Impacts of Columbia River Discharge on Salmonid Habitat: 1. A Nonstationary Fluvial Tide Model. *J. Geophys. Res.* 108 (C9), 3293. doi:10.1029/2002JC001382

LeBlond, P. H. (1978). On Tidal Propagation in Shallow Rivers. *J. Geophys. Res.* 83, 4717–4721. doi:10.1029/JC083iC09p04717

Liu, Y., Xia, X., Chen, S., Jia, J., and Cai, T. (2017). Morphological Evolution of Jinshan Trough in Hangzhou Bay (China) from 1960 to 2011. *Estuarine, Coastal Shelf Sci.* 198, 367–377. doi:10.1016/j.ecss.2016.11.004

Liu, Y., Ma, C., Fan, D., Sun, Q., Chen, J., Li, M., et al. (2018). The Holocene Environmental Evolution of the Inner Hangzhou Bay and its Significance. *J. Ocean Univ. China* 17 (6), 1301–1308. doi:10.1007/s11802-018-3562-2

Mei, X., Dai, Z., Wei, W., Li, W., Wang, J., and Sheng, H. (2018). Secular Bathymetric Variations of the North Channel in the Changjiang (Yangtze) Estuary, China, 1880-2013: Causes and Effects. *Geomorphology* 303, 30–40. doi:10.1016/j.geomorph.2017.11.014

Munk, W. H., and Cartwright, D. E. (1966). Tidal Spectroscopy and Predication. *Philo.Trans. R. Soc. (Ser. A)* 259, 533–581.

Pan, C., and Huang, W. (2010). Numerical Modeling of Suspended Sediment Transport Affected by Tidal Bore in Qiantang Estuary. *J. Coastal Res.* 26 (6), 1123–1132. doi:10.2112/jcoastres-d-09-00024.1

Pan, C.-H., Lin, B.-Y., and Mao, X.-Z. (2007). Case Study: Numerical Modeling of the Tidal Bore on the Qiantang River, China. *J. Hydraul. Eng.* 133, 130–138. doi:10.1061/(asce)0733-9429(2007)133:2(130)

Perillo, G. M. E. (1995). *Geomorphology and Sedimentology of Estuaries: Developments in Sedimentology*. Amsterdam: Elsevier Sci.

Pye, K., and Blott, S. J. (2014). The Geomorphology of UK Estuaries: The Role of Geological Controls, Antecedent Conditions and Human Activities. *Estuarine, Coastal Shelf Sci.* 150, 196–214. doi:10.1016/j.ecss.2014.05.014

Ralston, D. K., Talke, S., Geyer, W. R., Al-Zubaidi, H. A. M., and Sommerfield, C. K. (2019). Bigger Tides, Less Flooding: Effects of Dredging on Barotropic Dynamics in a Highly Modified Estuary. *J. Geophys. Res. Oceans* 124, 196–211. doi:10.1029/2018JC014313

Reddering, J. S. V., and Esterhuysen, L. (1989). Effects of River Floods on Sediment Dispersl in Small Estuaries: a Case Study from East London. *S. Afr. J. Geol.* 90, 458–470.

Sassi, M. G., and Hoitink, A. J. F. (2013). River Flow Controls on Tides and Tide-Mean Water Level Profiles in a Tidal Freshwater River. *J. Geophys. Res. Oceans* 118, 4139–4151. doi:10.1002/jgrc.20297

Savenije, H. H. G. (2012). *Salinity And Tides in Alluvial Estuaries*. Completely Revised 2nd edition. Available at: http://www.salinityandtides.com.

Talke, S. A., and Jay, D. A. (2020). Changing Tides: The Role of Natural and Anthropogenic Factors. *Annu. Rev. Mar. Sci.* 12 (1), 121–151. doi:10.1146/annurev-marine-010419-010727

Tu, J., Fan, D., and Voulgaris, G. (2021). Field Observations of Turbulence, Sediment Suspension, and Transport under Breaking Tidal Bores. *Mar. Geol.* 437 (3), 106498. doi:10.1016/j.margeo.2021.106498

Van Maren, D. S., Winterwerp, J. C., and Vroom, J. (2015). Fine Sediment Transport into the Hyper-Turbid Lower Ems River: The Role of Channel Deepening and Sediment-Induced Drag Reduction. *Ocean Dyn.* 65 (4), 589–605. doi:10.1007/s10236-015-0821-2

Wang, Z. B., Jeuken, M. C. J. L., Gerritsen, H., de Vriend, H. J., and Kornman, B. A. (2002). Morphology and Asymmetry of the Vertical Tide in the Westerschelde Estuary. *Cont. Shelf Res.* 22, 2599–2609. doi:10.1016/S0278-4343(02)00134-6

Wang, Z. B., Winterwerp, J. C., and He, Q. (2014). Interaction between Suspended Sediment and Tidal Amplification in the Guadalquivir Estuary. *Ocean Dyn.* 64, 1487–1498. doi:10.1007/s10236-014-0758-x

Wang, Z. B., Vandenbruwaene, W., Taal, M., and Winterwerp, H. (2019). Amplification and Deformation of Tidal Wave in the Upper Scheldt Estuary. *Ocean Dyn.* 69, 829–839. doi:10.1007/s10236-019-01281-3

Winterwerp, J. C., Wang, Z. B., Van Braeckel, A., Van Holland, G., and Kösters, F. (2013). Man-induced Regime Shifts in Small Estuaries-II: a Comparison of Rivers. *Ocean Dyn.* 63 (11-12), 1293–1306. doi:10.1007/s10236-013-0663-8

Xie, D.-f., and Pan, C.-h. (2013). A Preliminary Study of the Turbulence Features of the Tidal Bore in the Qiantang River, China. *J. Hydrodyn.* 25 (6), 903–911. doi:10.1016/S1001-6058(13)60439-4

Xie, D., Wang, Z., Gao, S., and De Vriend, H. J. (2009). Modeling the Tidal Channel Morphodynamics in a Macro-Tidal Embayment, Hangzhou Bay, China. *Continental Shelf Res.* 29, 1757–1767. doi:10.1016/j.csr.2009.03.009

Xie, D., Pan, C., Wu, X., Gao, S., and Wang, Z. B. (2017a). Local Human Activities Overwhelm Decreased Sediment Supply from the Changjiang River: Continued Rapid Accumulation in the Hangzhou Bay-Qiantang Estuary System. *Mar. Geology.* 392, 66–77. doi:10.1016/j.margeo.2017.08.013

Xie, D., Gao, S., Wang, Z. B., Pan, C., Wu, X., and Wang, Q. (2017b). Morphodynamic Modeling of a Large inside Sandbar and its Dextral Morphology in a Convergent Estuary: Qiantang Estuary, China. *J. Geophys. Res. Earth Surf.* 122 (8), 1553–1572. doi:10.1002/2017JF004293

Xie, D., Pan, C., Gao, S., and Wang, Z. B. (2018). Morphodynamics of the Qiantang Estuary, China: Controls of River Flood Events and Tidal Bores. *Mar. Geology.* 406, 27–33. doi:10.1016/j.margeo.2018.09.003

Xie, D., Wang, Z. B., Van der Wegen, M., and Huang, J. (2021a). Morphodynamic Modeling the Impact of Large-Scale Embankment on the Large Bar in a Convergent Estuary. *Mar. Geol.* 442, 106638. doi:10.1016/j.margeo.2021.106638

Xie, D. F., Wang, Z. B., Huang, J. B., and Zeng, J. (2021b). River, Tide and Morphology Interaction in a Macro-Tidal Estuary with Active Morphological Evolutions. *Catena*, major revised.

Zhang, X., Lin, C.-M., Dalrymple, R. W., Gao, S., and Li, Y.-L. (2014). Facies Architecture and Depositional Model of a Macrotidal Incised-valley Succession (Qiantang River Estuary, Eastern China), and Differences from Other Macrotidal Systems. *Geol. Soc. Am. Bull.* 126 (3/4), 499–522. doi:10.1130/B30835.1

Zhang, X., Dalrymple, R. W., Yang, S.-Y., Lin, C.-M., and Wang, P. (2015). Provenance of Holocene Sediments in the Outer Part of the Paleo-Qiantang River Estuary, China. *Mar. Geol.* 366, 1–15. doi:10.1016/j.margeo.2015.04.008

Zhang, M., Townend, I., Zhou, Y., and Cai, H. (2016). Seasonal Variation of River and Tide Energy in the Yangtze Estuary, China. *Earth Surf. Process. Landforms* 41 (1), 98–116. doi:10.1002/esp.3790

Conflict of Interest: The authors declare that the research was conducted in the absence of any commercial or financial relationships that could be construed as a potential conflict of interest.

Publisher's Note: All claims expressed in this article are solely those of the authors and do not necessarily represent those of their affiliated organizations, or those of the publisher, the editors, and the reviewers. Any product that may be evaluated in this article, or claim that may be made by its manufacturer, is not guaranteed or endorsed by the publisher.